CONF-920631--35

DE92 014411

AN EVALUATION OF ANALYSIS METHODOLOGIES FOR PREDICTING CLEAVAGE ARREST OF A DEEP CRACK IN AN RPV SUBJECTED TO PTS LOADING CONDITIONS*

J. Keeney-Walker and B. R. Bass
Oak Ridge National Laboratory
Oak Ridge, Tennessee

ABSTRACT

Several calculational procedures are compared for predicting cleavage arrest of a deep crack in the wall of a prototypical reactor pressure vessel (RPV) subjected to pressurized-thermal-shock (PTS) types of loading conditions. Three procedures examined in this study utilized the following models: (1) a static finite-element model (full bending); (2) a radially constrained static model; and (3) a thermoelastic dynamic finite-element model. A PTS transient loading condition was selected that produced a deep arrest of an axially-oriented initially shallow crack according to calculational results obtained from the static (full-bending) model. Results from the two static models were compared with those generated from the detailed thermoelastic dynamic finite-element analysis. The dynamic analyses modeled cleavage-crack propagation using a node-release technique and an application-mode methodology based on dynamic fracture toughness curves generated from measured data. Comparisons presented here indicate that the degree to which dynamic solutions can be approximated by static models is highly dependent on several factors, including the material dynamic fracture curves and the propensity for cleavage reinitiation of the arrested crack under PTS loading conditions. Additional work is required to develop and validate a satisfactory dynamic fracture toughness model applicable to postcleavage arrest conditions in an RPV.

INTRODUCTION AND BACKGROUND

Analysis of pressurized-thermal-shock (PTS) events in reactor pressure vessels (RPVs) requires an understanding of conditions that govern initiation, rapid propagation, arrest, and ductile tearing of cracks. In PTS scenarios, inner-surface cracks in an RPV have the greatest propensity to propagate because they are located in the region of highest thermal stress, lowest temperature and greatest irradiation damage. If such a crack begins to propagate radially through the vessel wall, it will extend into a region of higher fracture toughness due to the higher temperatures and less irradiation damage. Because a finite probability exists that crack initiation will occur in a PTS transient, assessment of vessel integrity requires the ability to predict all phases of a fracture event. This paper examines several of the issues related to developing and evaluating fracture mechanics methodologies that can be used for performing these assessments. Specifically, procedures for predicting cleavage arrest and reinitiation of a deep crack in the wall of an RPV are considered, including circumstances under which certain quasi-static methods can be used to approximate results from dynamic formulations. Levels of conservatism associated with applications of these methodologies to code-based analyses of RPVs will also be discussed.

Based on results from the Integrated Pressurized-Thermal-Shock (IPTS) Program [1-3] and other studies, the Nuclear Regulatory Commission (NRC) established the PTS rule (10 CFR 50.61) [4] to insure the integrity of RPVs under PTS transients. Plant-specific analyses must be performed for any plant that is intended to operate beyond the screening criteria. Furthermore, *Regulatory Guide 1.154* [5] provides guidance on the methodology for performing plant-specific safety analyses, including references to the IPTS study as an acceptable methodology for the probabilistic fracture-mechanics (PFM) portion of the analyses.

A typical quasi-static methodology for performing deterministic and probabilistic fracture mechanics analyses is embodied in the OCA-P computer program [6], which is referenced in the IPTS study. The OCA-P program was developed at ORNL specifically for simulating the cleavage fracture response of an RPV subjected to a PTS event. The program is based on linear-elastic fracture-mechanics (LEFM) theory and on a static equilibrium description of the crack propagation/arrest events in an RPV. As a consequence of the static model, any dynamic effects associated with events in an RPV are excluded from OCA-P analyses. Generally, it is perceived that the OCA-P approach produces conservative cleavage fracture predictions, even though the dynamic effects of a complete crack propagation event (involving interaction of cleavage and ductile modes of fracture) are not precisely understood. It should be observed that the current version of OCA-P also excludes from the analysis the possibility of pre-cleavage ductile tearing. (Such events were demonstrated in the second HSST pressurized-thermal-shock test, PTSE-2 [7].)

Several recent studies [8,9] have suggested that the methodology incorporated into OCA-P for predicting crack arrest (i.e. LEFM principles and static equilibrium assumptions) may be overly conservative when used in conjunction with the American Society of Mechanical Engineers Boiler and Pressure Vessel Code *(ASME Code*, Section XI [10]). Specifically, results from dynamic calculations are used in Refs. 8 and 9 to argue that currently accepted ASME code procedures are overly conservative in crack arrest predictions for the case where an initially shallow crack arrests deep in the wall of a vessel. The argument is based on the observation that the time interval for crack propagation is considerably less than the fundamental period of the structural response. In particular, the bending response of the structure that provides additional loading of a deep arrested crack in a condition of static equilibrium is small during the crack propagation event; bending does not develop until well after crack arrest has occurred. Consequently, analyses such as those performed with OCA-P, which incorporate influence coefficients based on full bending of the structure, predict larger crack extensions and a higher required material toughness for crack arrest than would be predicted by a dynamic analysis.

In the following sections, several of these issues are examined quantitatively through static and dynamic analyses of a hypothetical RPV subjected to a PTS transient. Static analyses were performed with the OCA-P code to identify shallow cracks that initiate in cleavage and arrest deep in the wall of the RPV. The OCA-P predictions are compared with application-mode dynamic analysis results based on postulated dynamic fracture toughness models generated in the Heavy-Section Steel Technology (HSST) wide-plate testing program [11,12]. The propensity for cleavage reinitiation of the arrested cracks is investigated using both static and dynamic initiation toughness relations. A radially constrained static model [13] developed to approximate boundary conditions from the dynamic model at the time of crack arrest is applied to the same PTS transient, and the results are compared with those from the dynamic analyses. Finally, some observations are made concerning important issues that have been identified for further development.

ANALYSIS TECHNIQUES

Static Full Bending Model

The thermal, stress, and fracture-mechanics analyses in the OCA-P computer program are performed in various analytical steps. The specified transient, which consists of the reactor primary-system pressure and the reactor vessel downcomer coolant temperature as functions of time, is the input to OCA-P. The coolant temperature and a specified time-dependent fluid-film heat-transfer coefficient are used in OCA-P for a one-dimensional (1-D) thermal analysis to obtain the radial temperature distribution in the vessel wall as a function of time. Radial variations in material thermal properties are permitted, and thus cladding can be treated as a discrete region. Also, as an option to calculating the wall temperatures with OCA-P, these temperatures can be obtained by other means and then used as input to the program.

Once the wall temperatures have been determined, OCA-P performs a 1-D stress analysis for the unflawed vessel to obtain the circumferential and longitudinal pressure and thermal stresses as functions of time and radial position in the wall. If, however, the stresses are available from another source, they can be used as input rather than calculated.

The stress-intensity factors (K_I) are calculated using a superposition technique that makes use of influence coefficients based on a 90° model and the above stresses, as described in Ref. 6. The calculated K_I values are obtained as functions of crack depth and time in the transient. In a deterministic analysis, values of the static crack initiation toughness (K_{Ic}) and the crack-arrest toughness (K_{Ia}) are also evaluated as a part of the fracture-mechanics analysis for all crack depths and times in the transient. A comparison of K_I with K_{Ic} and K_{Ia} permits an evaluation of flaw behavior.

Static Constrained Model

Fabi and Ayres [13] argue that the structural response of an RPV is slow compared to the time of cleavage crack extension, and that the crack extends into a vessel which is, to a considerable degree, constrained from motion by its inertia and has not responded to the new crack geometry. The conditions on the boundary remote from the crack are essentially the same as those existing prior to crack extension, i.e., the crack loading is displacement controlled for the short time prior to and during arrest. It would appear, therefore, that a static analysis with the appropriate displacement control would enable a simple calculation of the K_I at crack arrest. In order to find appropriate loading conditions, it is necessary to determine the nature of the motion of the vessel during the dynamic crack-extension event. Results of dynamic analyses presented in Ref. 13 imply that the motion of the point on the outside surface of the vessel near the plane of the crack during the time of crack extension is a very small part of the eventual peak motion. Also, the time of the peak motion response corresponds to the time of the peak crack-tip response. Thus, the stress-intensity factor during the crack extension is approximated in Ref. 13 by a static elastic finite element analysis performed for the various crack lengths, but assuming that the outer surface of the vessel does not move radially from its position at the beginning of crack extension.

To take account of the post-arrest motion of the vessel which would increase the load on the crack, the restraints are removed from the static model to compute K_I at the crack tip. The peak K_I due to the load up after arrest is predicted by multiplying the statically computed K_I by a dynamic amplification factor determined from dynamic analyses of similar structures. This factor was estimated to be 1.2 for an RPV in Ref. 9. The resulting K_I is used to estimate if reinitiation would occur by comparing it to the appropriate initiation toughness value. The procedure was applied to a series of crack initiation and arrest events in the ORNL wide-plate tests in Ref. 13.

Dynamic Analysis Techniques

Thermoelastic dynamic analyses described in this paper were carried out using an ORNL modified version of ADINA [14,15] for dynamic crack analysis. The modified ADINA code is capable of performing both application- and generation-mode dynamic analyses. In the application-mode analysis, the crack tip is propagated incrementally when K_I, the dynamically computed stress-intensity factor, equals the specified dynamic fracture toughness value, K_{ID}. In the generation-mode analysis, the crack tip is propagated incrementally according to a prescribed crack position vs. time relationship, with the values of fracture toughness determined from the dynamically computed K_I. For both modes, the dynamic stress-intensity factor is determined in each time step from the dynamic J-integral containing the appropriate inertial and thermal terms. The crack-growth modeling technique of modified ADINA is based on that of Ref. 16, in which the finite element immediately ahead of the crack tip is

divided into N subelements (typically, N = 5–10). During propagation, the tip is moved through these subelements along the crack plane in discrete jumps. The position of the crack tip relative to these subelement divisions is determined from restraining forces which are placed on the crack-plane nodes of the element adjacent to the crack tip; these forces are postulated to vary linearly with crack tip location within the element and are released incrementally as the tip propagates through the element.

The application-mode analyses of the present study employed two empirical dynamic fracture toughness relations which were developed in support of the HSST wide-plate testing program [11]. The first of these relations (pretest model) was developed by Kanninen et al. [17] from Japanese wide-plate data [18] primarily for use in pretest planning analysis of the wide-plate experiment. The relation, detailed in Ref. 19, is taken to have the form

$$K_{Id} = K_{Ia} + A(\dot{a})^2 , \text{ where} \tag{1}$$

$$K_{Ia} = 29.5 + 1.344 \exp [0.0261(T - RT_{NDT} + 160)], \text{ and} \tag{2}$$

$$A(T) = [329.7 + 16.25 (T - RT_{NDT})] \times 10^{-6} , \text{ or} \tag{3}$$

$$A(T) = [121.71 + 1.2962 (T - RT_{NDT})] \times 10^{-6} , \tag{4}$$

if $(T - RT_{NDT})$ is greater or less than $-13.9°C$, respectively. Units for K, A, $\dot{a}$, and T are MPa m$^{1/2}$, MPa s^2 m$^{-3/2}$, m/s and °C, respectively. In Eq. (1), it is assumed that the equation for K_{Ia} can be chosen independently; here K_{Ia} represents the ASME Section XI lower bound toughness curve [10].

The second relation (posttest model) was developed by Schwartz [12] from dynamic data generated in the WP-1 series of HSST wide-plate tests, which employed specimens fabricated from good-quality A 533 grade B class 1 steel. In Ref. [12], a linear form was assumed for the K_{ID} ($\dot{a}$, T) relation, the coefficients of which were estimated from test data using generation-mode computational methodology. The resulting function is given by

$$\dot{a} = C_0(T) + C_1(T) \times (K_I/K_{Ia}) \quad K_I/K_{Ia} \geq 1 \tag{5}$$

$$\dot{a} = 0 \quad K_I/K_{Ia} < 1 \tag{6}$$

where the temperature-dependent coefficients C_0 and C_1 are in m/s and have the functional form depicted in Fig. 1, and K_{Ia} is taken to be the ASME Section XI lower bound crack arrest toughness curve [10]. In Ref. 12, the relation given by Eqs. (5)-(6) was successfully applied to a wide-plate experiment [12, 20] that was not included in the data base used to derive the model. In Reference 20, the two fracture toughness relations were used to analyze wide plate test WP-1.7. The two measured crack lengths at arrest were 0.528 and 0.635 m. The pretest model predicted arrest at a crack length of 0.666 m whereas the posttest model predicted arrest at a crack length of 0.538 m, which is close to the first measured arrest value.

PROBLEM DEFINITION

The PTS event selected for analysis from the USNRC/IPTS studies is the H. B. Robinson transient 922.B [1] (modified for a constant value of the heat transfer coefficient and depicted in Fig. 2). The geometry of the vessel is given in Table 1, the mechanical and fracture properties in Table 2, and the thermophysical properties in Table 3. The PTS shift equation for ΔRT_{NDT} described in Table 2 is given by:

$$\Delta RT_{NDT} = 0.56(38.0 + 470.0 \times Cu + 350.0 \times Cu \times Ni)(F \times 10^{-19})^{0.27}, \tag{7}$$

and

$$F = F_0 e^{(-0.0094 \times a)} \tag{8}$$

where, ΔRT_{NDT} is in °C, F is the attenuated fluence, F_0 is the fluence at the inner surface of the RPV, and a is the crack depth in mm.
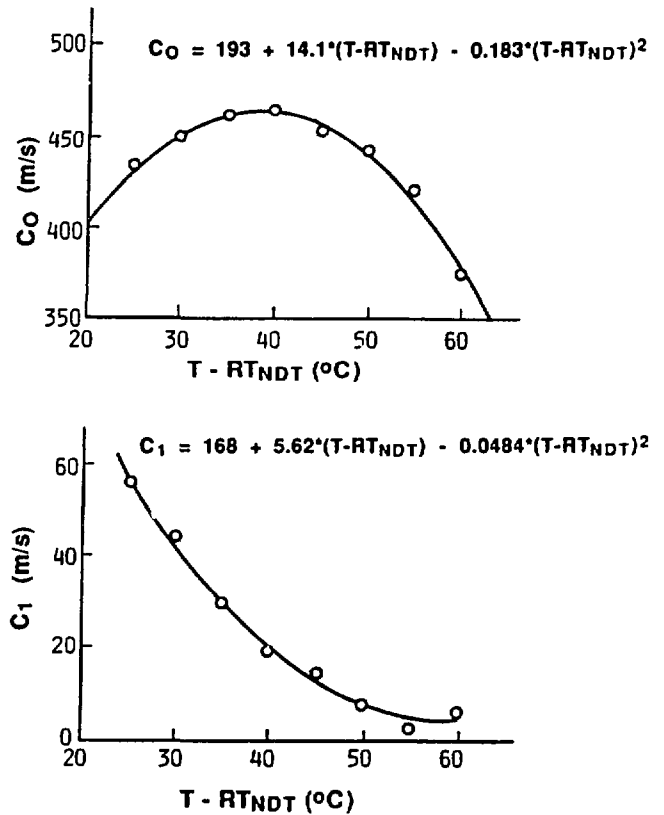

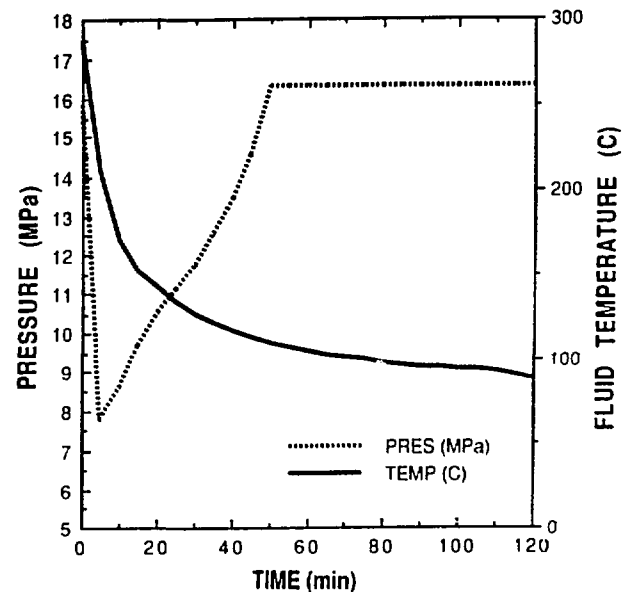Fig. 1 Temperature dependence of crack-speed regression coefficients.

Fig. 2 Pressure and temperature time histories based on the H. B. Robinson transient 9.22B.

Table 1. Geometry of vessel used in PTS analysis

Inner vessel radius	1981.2 mm	(78.0 in.)
Wall thickness (with cladding)	236.474 mm	(9.31 in.)
Cladding thickness	5.587 mm	(0.22 in.)

Table 2. Mechanical and fracture toughness properties of pressure vessel materials

	Cladding	Base Metal
Modulus of Elasticity (E)	1862000 MPa (27000 ksi)	193100 MPa (28000 ksi)
Poisson's ratio (υ)	0.3	0.3
Thermal expansion coefficient (α)	1.782E-5/C (9.9E-6/F)	1.44E-5/C (8.00E-6/F)

- Fracture toughness curves: ASME lower-bound K_{Ic} and K_{Ia} curves.
- $RT_{NDT_0} = -17.7°C$ (0°F).
- Fluence at inner vessel wall surface = 3.15E+19 n/cm^2.
- ΔRT_{NDT} predicted by PTS shift equation [see Eq. (7) in text].
- Fluence attenuation constant = 0.0094 mm^{-1} (0.24 $in.^{-1}$).
- Copper (Cu) = 0.22 weight %.
- Nickel (Ni) = 0.80 weight %.

Table 3. Thermophysical properties of pressure vessel materials

|	Cladding	Base Metal
Thermal Conductivity (k)	17.3 watt/m-C (10 BTU/hr-ft-F)	41.52 watt/m-C (24 BTU/hr-ft-F)
Specific Heat (c_p)	502 Joule/kg-C (0.12 BTU/lb-F)	502 Joule/kg-C (0.12 BTU/lb-F)
Density (ρ)	7830 kg/m^3 (489 lb/ft^3)	7830 kg/m^3 (489 lb/ft^3)

Initial vessel temperature: 288°C (550°F)

Coefficient of convective heat transfer: 2270 watt/m^2-C (400 BTU/hr-ft²-F)

Based on an OCA-P analysis, an infinitely long flaw having a depth of a_0 = 0.024 m (a/w= 0.10) is predicted to initiate in cleavage at time t = 36 min and to arrest at a depth of a_f = 0.119 m (a/w = 0.50). The hoop stress and temperature distributions through the vessel wall at the time of the crack run/arrest event are depicted graphically in Fig. 3. In Fig. 4, crack initiation is predicted to occur at the intersection points of the applied K_I and the K_{Ic} toughness curves. Crack arrest occurs at the intersection point of the applied K_I and the K_{Ia} toughness curves shown in Fig. 5.
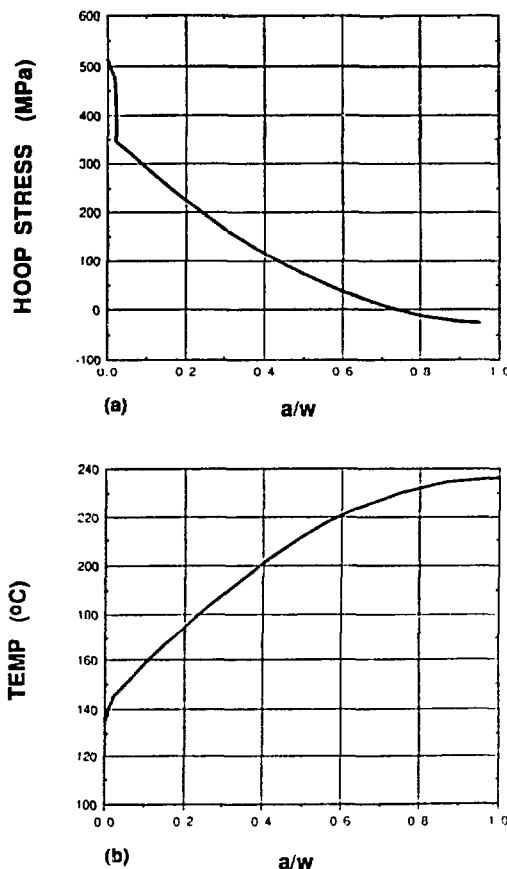
Fig. 3 Hoop stress and temperature distributions through the vessel wall at time t = 36 min: (a) hoop stress; (b) temperature.
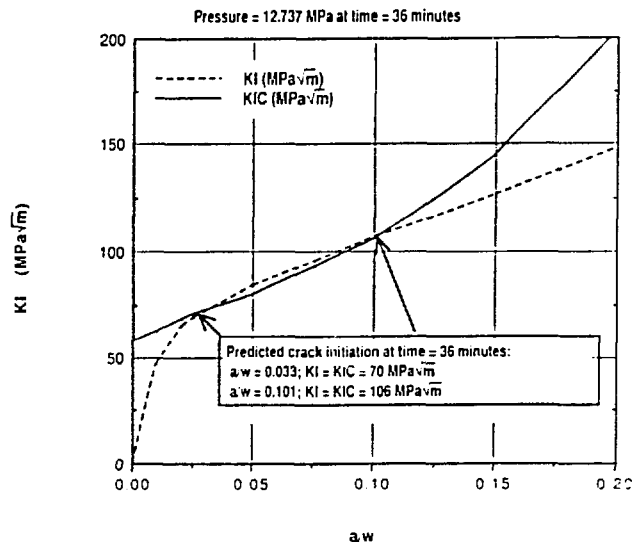
Fig. 4 Predicted crack initiation in PTS transient.

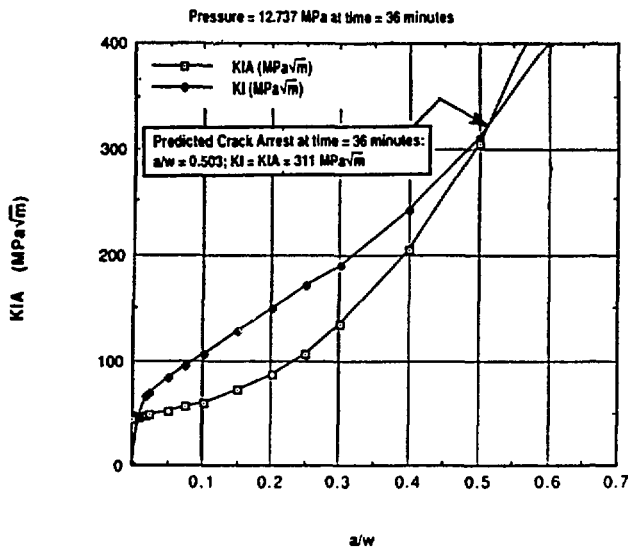Pressure = 12.737 MPa at time = 36 minutes

Fig. 5   Predicted crack arrest in PTS transient.

FINITE ELEMENT FRACTURE ANALYSES

Finite Element Model

In the static and dynamic thermoelastic analyses, a 2-D plane strain finite-element formulation was utilized to model the test vessel. The finite element model employed in these analyses is depicted in Fig. 6 and consists of 1994 nodes and 613 eight-noded isoparametric elements. The material properties given in Table 2 were assumed to be constant. A 2×2 numerical integration order was used in all the analyses. The values of the radial temperature distribution and internal pressure at the time of cleavage crack propagation for this transient (t = 36 min) were used as the boundary conditions and assumed to be constant during the run-arrest event. The pressure at crack initiation of 12.737 MPa was
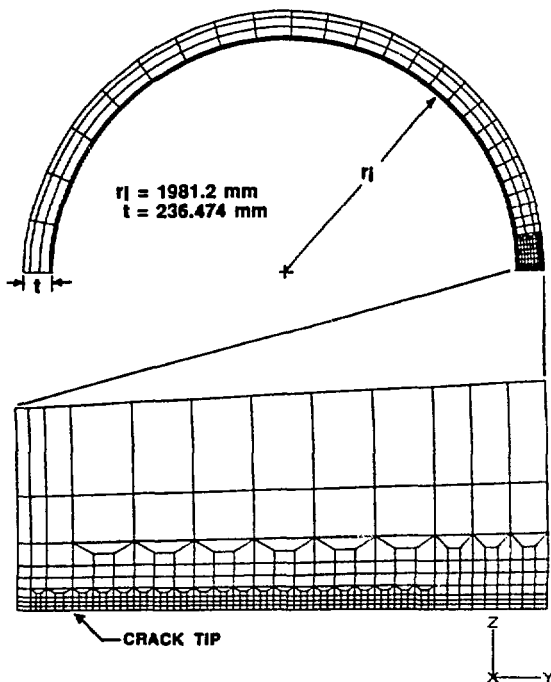

Fig. 6   Finite element model of the RPV.

applied to the model using 2-D element pressure surfaces. In order to provide the proper constraint for the thermal stresses, the material stress-free temperature was lowered to 184°C (reference temperature is 288°C) to produce a mean out-of-plane stress through the vessel wall that approximated an axial stress given by the relation (Pr/2t). The boundary conditions of the constrained model were applied on the outer edge of vessel as fixed displacements in the radial direction, corresponding to the y displacement of the outer corner at initiation.

Static Analysis (Full Bending)

Initially, quasi-static analyses were performed with the modified ADINA program for the initial crack depth (a/w = 0.10) and for two other crack depths (a/w = 0.49 and a/w = 0.51) which bound the arrest location determined by OCA-P. The computed K_I values compare well with the OCA-P calculations (for a/w = 0.10, K_I = 106 MPa·√m̄ (ADINA) and 106 MPa·√m̄ (OCA-P); for a/w = 0.50, K_I = 316 MPa·√m̄ (ADINA), 311 MPa·√m̄ (OCA-P)), and are reported in Table 4.

Application-Mode Dynamic Analysis

The first application-mode dynamic analysis was performed using the ASME Section XI lower bound toughness curves [10]. Equation 2 was used to calculate K_{Ia} and the following equation was used to calculate K_{Ic}:

$$K_{Ic} = 36.5 + 3.084 \exp [0.036(T - RT_{NDT} + 100)] \quad (9)$$

In this case, the crack was assumed to arrest if K_{Id} fell below K_{Ia} or if the crack velocity dropped below a threshold velocity of 2% of the shear wave velocity (~60 m/s). The assumption that the crack will not propagate at a slow speed is supported by analyses of the wide plate tests [11]; in principle, the abrupt stopping of crack extension provides a better correlation with observed results. In Ref. 20, the velocity of the crack, which is measured by strain gages, ranged from 200 to 500 m/s prior to arrest for WP-1.7.

Analysis results predicted crack arrest at a/w = 0.358 for the pretest fracture toughness model given by Eqs. (1)-(4) (path A to B in Fig. 7) and at a/w = 0.31 for the posttest model of Eqs. (5)-(6) (path A to D in Fig. 7). After the initial arrest, K_I oscillates due to vessel bending and reaches peak values of 262 MPa·√m̄ at 19.5 ms (point C in Fig. 7) and 209 MPa·√m̄ at 2.9 ms (point E in Fig. 7) for the pretest and posttest models, respectively. If crack reinitiation is assumed to occur when the applied K_I increases above the static K_{Ic} value calculated from Eq. (9), then the results depicted in Fig. 7 do not predict reinitiation for either of the fracture toughness models.

In general, the lower-shelf and transition fracture toughness of structural steels decreases with increasing loading rate. So for any given temperature, the fracture toughness measured in a high rate loading test, K_{Id}, is generally lower than the fracture toughness measured in a static test, K_{Ic}. Typically, dynamic K_{Ic} tests [21] are conducted at crack-tip strain rates at the elastic-plastic boundary varying between 10 and 40/sec ($\dot{K}$ between 10^5 and 3×10^5 MPa·√m̄/sec), whereas static K_{Ic} tests are conducted at strain rates at approximately 10^{-5}/sec ($\dot{K} \approx 3 \times 10^2$ MPa·√m̄/sec).

A procedure was developed for this study to estimate the dynamic initiation toughness from measured data in four steps: (1) a representative high loading rate, $\dot{K}$, can be determined from the slope of K_I vs. time curve generated

Table 4. Results of static and application-mode dynamic analyses

Analysis	a/w	Temp (°C)	Time (ms)	K_I (MPa·√m)	Event	Note
Static						
Full bending	.10	158		106	Initiation	
	.50	210		316	Arrest	
Radially constrained	.10	158		106	Initiate	
	.30	187		130	Arrest	
	.30	187		200	Reinitiate	
Dynamic						
Pretest model – LB[a]	.10	158	0.00	106	Initiate	$\dot{a}$ = 250 m/s
Eqs. (1)–(4)	.358	195	0.47	174	Arrest	$\dot{a}$ < 50 m/s
	.358	195	19.50	262	Reinitiate	$\dot{a}$ = 225 m/s
	.46	207	19.70	261	Arrest	$\dot{a}$ < 50 m/s
			24.50	335	Peak	K_I = 410 to rein
Posttest model – LB[a]	.10	158	0.00	106	Initiate	$\dot{a}$ = 525 m/s
Eqs. (5)–(6)	.31	189	0.15	135	Arrest	$K_I < K_{Ia}$
	.31	189	2.90	209	Reinitiate	$\dot{a}$ = 200 m/s
	.36	196	3.02	202	Arrest	$\dot{a}$ < 50 m/s
			19.30	263	Peak	K_I = 264 to rein
Posttest model – LB[b]	.10	158	0.00	106	Initiate	$\dot{a}$ = 525 m/s
	.31	189	0.15	135	Arrest	$K_I < K_{Ia}$
			19.30	236	Peak	K_I = 254 to rein
Pretest model – MEAN[a]	.10	158	0.00	106	Initiate	$\dot{a}$ = 192 m/s
	.28	185	0.36	154	Arrest	$\dot{a}$ < 50 m/s
			19.40	208	Peak	K_I = 256 to rein
Posttest model – MEAN[a]	.10	158	0.00	106	Initiate	$\dot{a}$ = 511 m/s
	.23	178	0.08	119	Arrest	$K_I < K_{Ia}$
			19.20	180	Peak	K_I = 200 to rein

[a] K_{Id} calculated from extrapolated material property data and K_{Ic} curve.
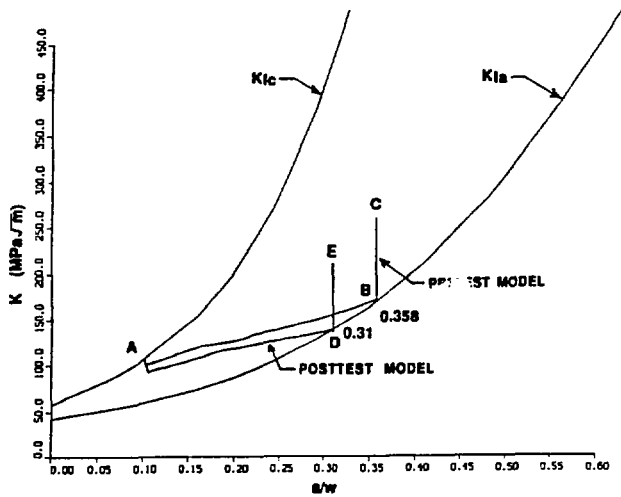[b] K_{Id} calculated from 30°C temperature shift in K_{Ic} curve.
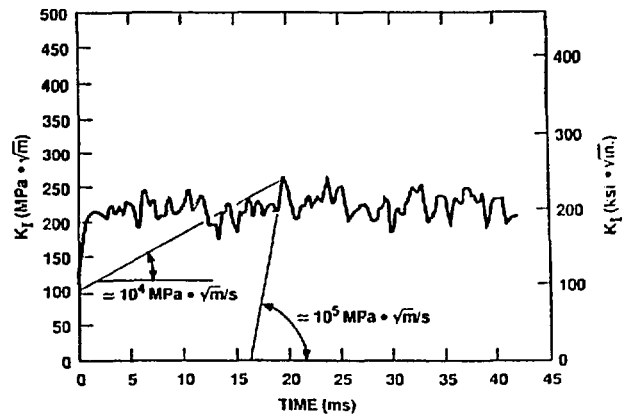

Fig. 8 $\dot{K}$ obtained from slope of K_I vs. time for application-mode dynamic analysis.
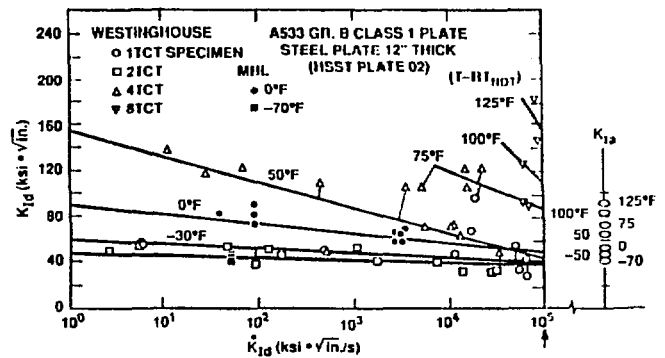

Fig. 9 K_{Id} vs. $\dot{K}_{Id}$ for A533B at several temperatures. *Source:* W. O. Shabbits, *Dynamic Fracture Toughness Properties of Heavy Section A 533 Grade B Class 1 Steel Plate,* Westinghouse R&D Center, WCAP-8623, HSST Technical Report No. 13, December 1970.

Table 5. Values for K_{Id} at various temperatures for a loading rate ($\dot{K}$) of 10^5 MPa √m/sec (10^5 ksi √in./sec)

T-RT_NDT [°C (°F)]	K_Id [MPa √m (ksi √in.)]	a/w
0 (0)	55 (50)	0.00
42 (75)	97 (88)	0.13
56 (100)	123 (112)	0.20
69 (125)	169 (154)	0.26

Fig. 7   K vs. a/w for application-mode dynamic analysis.

from a dynamic analysis; (2) at this $\dot{K}$, the K_{Id} vs. temperature (T-RT_NDT) relation can be determined from measured data; (3) the relation of (T-RT_NDT) vs. a/w is determined for this material from the PTS transient at crack initiation; (4) a K_{Id} vs. a/w curve can be constructed from curves generated in steps (2)–(3). The applied K_I vs. time curve is shown in Fig. 8 for the application-mode dynamic analysis with two representative loading rates ($\dot{K}$) of 10^4 and 10^5 MPa·√m/sec. Values of K_{Id} at a $\dot{K}$ of 10^5 MPa·√m/sec (10^5 ksi·√in./sec) for A533 Grade B Class 1 steel at several temperatures (T-RT_NDT) are obtained from Fig. 9 [22] and listed in Table 5. From the reference temperature vs. a/w

relation shown in Fig. 10, the initiation toughness was determined for the selected values of a/w tabulated in Fig. 11. The K_{Id} curve in Fig. 11 is constructed from a curve fit to the K_{Id}/K_{Ic} values in the table of Fig. 11 using the relation

$$K_{Id}/K_{Ic} = A \exp (B \cdot a/w) \qquad (10)$$

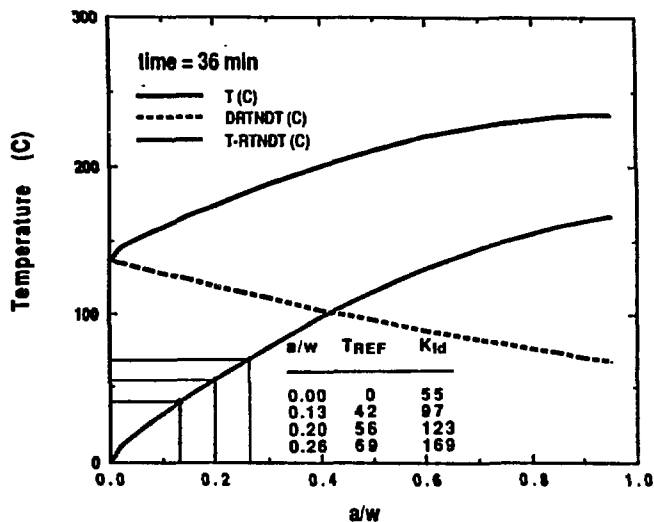where A is 0.923454, B is –2.10665 and K_{Ic} is given by Eq. (9).

Fig. 10 Temperature vs. a/w for analysis.

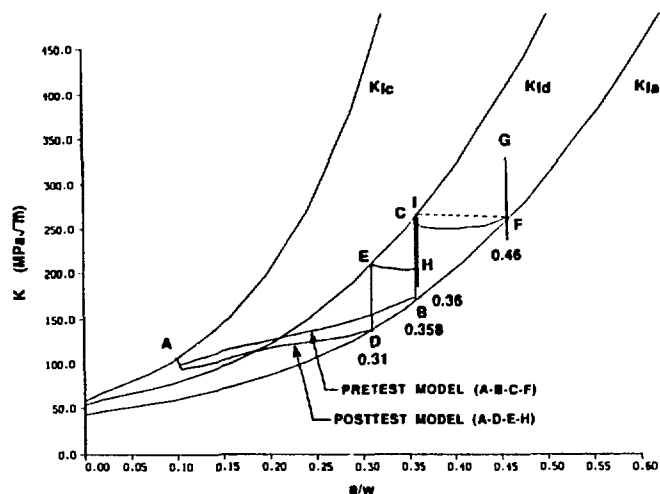Fig. 11 Fracture toughness vs. a/w for analysis.

Fig. 12 K vs. a/w for application-mode dynamic analyses using the initiation toughness curve generated from the ASME lower bound K_{Ic} curve.
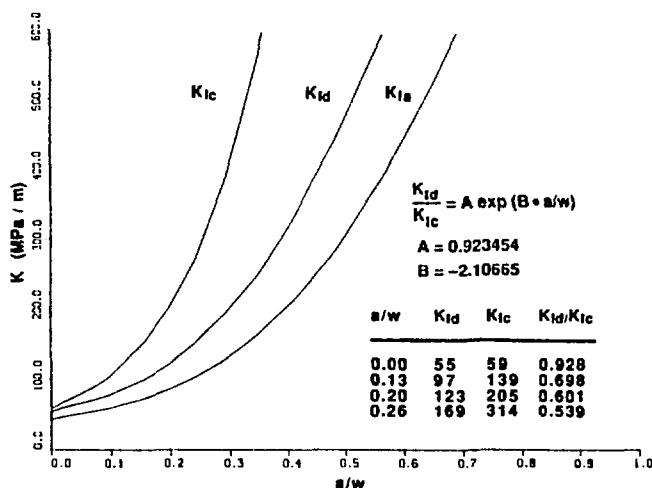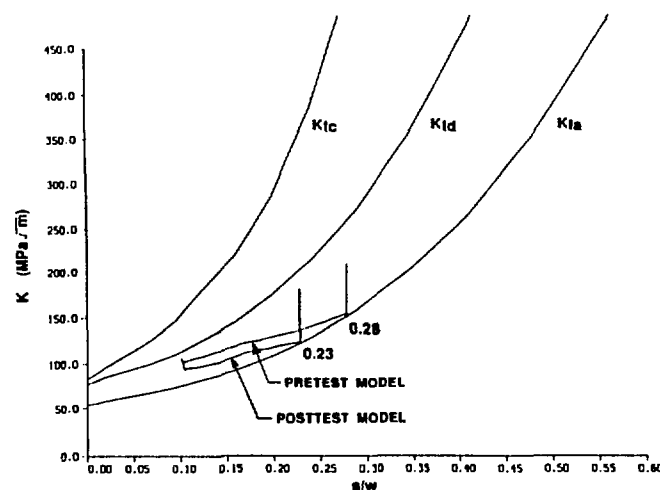

Fig. 13 K_I vs. a/w for application-mode dynamic analyses using the initiation toughness curve generated from an estimated mean K_{Ic} curve.

The application-mode dynamic analyses were repeated using the generated K_{Id} curve in place of the ASME lower bound K_{Ic} curve to determine the propensity for crack reinitiation. As shown in Fig. 12, the crack reinitiated for the pretest model at a K_I value of 262 MPa•√m̄, and then arrested at a K_I of 261 MPa•√m̄ and a/w of 0.46 (path A-B-C-F). After arrest K_I again oscillates with a peak value of 335 MPa•√m̄ at 24.5 ms (point G) which is below the K_{Id} curve. For the posttest model, the crack reinitiated and arrested because of low velocity at an a/w of 0.36 (path A-D-E-H). KI reached a peak value of 263 MPa•√m̄ at 19.3 ms (point I), which missed the reinitiation value by 1 MPa•√m̄. If reinitiation had occurred, the crack would have arrested at an a/w of approximately 0.46 which is consistent with the OCA-P prediction. This is shown as a dashed line in Fig. 12.

When the application-mode analyses were repeated using estimated mean curves for K_{Ic} and K_{Ia} (obtained from the ASME lower bound K_{Ic} and K_{Ia} curves), both the pretest and posttest fracture toughness models produced arrest at shallower depths, a/w = 0.28 and 0.23, respectively; the cracks did not reinitiate. These results are depicted in Fig. 13. Data from Ref. 22 imply that an initiation toughness

curve valid for high loading rates could be generated by shifting the lower bound K_{Ic} curve 30°C to the right: application-mode analyses based on this shifted curve resulted in no reinitiation. Results of these dynamic analyses are reported in Table 4.

Static Analysis (Radially Constrained Outer Edge)

As discussed earlier, it has been proposed [13] that the stress-intensity factor during crack extension can be approximated by a static analysis which assumes that the vessel is essentially stationary. The technique proposed in Ref. 13 was investigated in the present study through an application to the same RPV model and PTS loading transient defined earlier. A series of static thermoelastic analyses were performed at various crack lengths, with the vessel fixed radially on the outer surface at the radial displacement calculated for the initial crack depth. The results of these analyses are depicted in Fig. 14, where the calculated K_I values from OCA-P (static-full bending), application-mode dynamic analysis (posttest model and K_{Id} curve), and static (radially constrained outer surface) are plotted as functions of a/w.
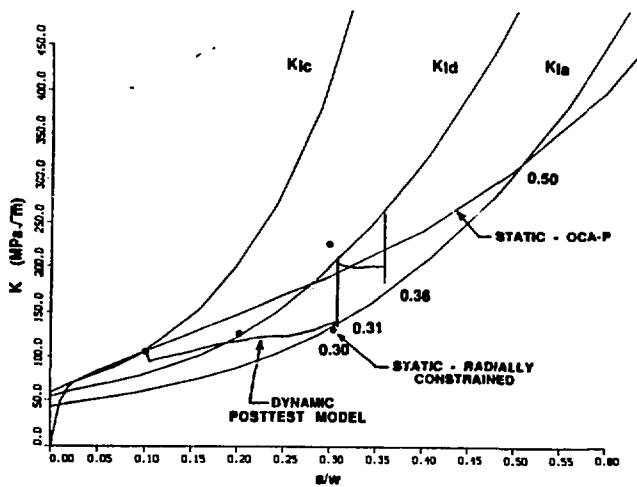
Fig. 14 Comparison of K vs. a/w for the static and application-mode dynamic analyses.

Note that the K_I computed from the static radially constrained model intersects the K_{Ia} curve at about the same point as the first arrest of the application-mode dynamic analysis using the posttest model (3% difference). The unconstrained value of K_I at an a/w of 0.30 is 188 MPa·√m, and when this value is amplified by 1.2 the K_I value is 226 MPa·√m which would predict reinitiation since K_{Id} is 200 MPa·√m. Analyses to determine subsequent crack propagation and rearrest were not completed for inclusion in this paper due to time constraints. A comparison of predicted crack arrest values for some of the previously described analyses is also depicted in Fig. 14. The differences in these results are clearly dependent upon whether or not the crack reinitiates.

DISCUSSION OF RESULTS

The near-term (i.e., a few ms after the previous arrest) reinitiation of a crack is determined by the dynamic loading on the crack and the material toughness. The thermoelastic dynamic analyses predict rapid oscillations in the applied K_I about a value above 200 MPa·√m following the initial cleavage arrest, with loading rates on the crack that may be on the order of 10^4 or 10^5 MPa·√m/sec. At these K_I levels, significant plasticity may be occurring in the crack-tip region, which is not considered in the present analyses; furthermore, the strain-rate dependence of plasticity in A 533 B steel has been well established (see Ref. 23). While strain-rate dependent plasticity effects in dynamic fracture of A 533B steel have been studied extensively (for example, see Ref. 15), these models are not sufficiently developed or validated for applications to the present study.

An important related factor is that toughness appears to be very sensitive to loading rate, as depicted in Fig. 9. The data in Fig. 9 were obtained with CT specimens loaded from essentially no load to failure at a fairly uniform loading rate. Studies [13] of crack reinitiation in the Electric Power Research Institute/Combustion Engineering moment modified compact tension tests and the HSST wide-plate tests imply that reinitiation K_I values were higher than would be predicted by Fig. 9. Therefore, for PTS-type loadings or loading in a large structure, some other mechanism may be acting that would call into question the transfer of the phenomena of Fig. 9 to the larger test structure situations. Some research which has been performed to study the nature and reason for rate effects on initiation values [24] suggests

that there may be an incubation time required for dynamic initiation. In order to assess the relevance of the Fig. 9 data, substantial work may be required.

The analyses discussed above provide what is probably a lower bound estimate of the influence of vessel dynamic response on crack arrest. The plane-strain analysis model of Fig. 6 incorporates the assumption of an infinite flaw length. Prior analyses [25] have shown that the stress-intensity factor at the deepest point of a semielliptical surface crack remains less than that for an infinite flaw even when the flaw surface dimension becomes very long. The stress-intensity factor time history for the period following the initial crack arrest will therefore be conservative for flaws of finite length. Incorporation of finite length flaw stress-intensity factors into the analysis, together with a statistical rather than a lower-bound representation of K_{Ic}, would probably preclude crack reinitiation in many cases. The initial crack arrest would then become the final arrest at that time in the PTS transient.

The analysis results of Fig. 14 show that without reinitiation, the crack depth to vessel-wall thickness ratio (a/w) at arrest would be 0.31 (posttest model) rather than the value of 0.5 predicted by the OCA-P static equilibrium model. This difference could be very important in a probabilistic fracture mechanics analysis since, beyond a critical depth, the arrested cleavage crack becomes unstable due to the onset of ductile tearing.

Another post-arrest consideration is the effect of high-pressure transients, which have been determined to be the most probable from the IPTS studies. In these transients, K_I can exceed K_{Ic} for deeper crack depths, increasing the probability of crack reinitiation at a later time in the transient. Thus, even if an initial cleavage crack arrest takes place as a result of dynamic effects, a series of reinitiation/arrest events can lead to vessel failure.

SUMMARY AND CONCLUSIONS

Comparisons of crack arrest predictions from the static and dynamic analyses indicate that the radially-constrained static model shows good agreement with the posttest dynamic model for the initial crack arrest depth, while the full-bending static model (OCA-P) leads to an over-prediction of the first and second arrest depth. The magnitude of these differences is dependent upon whether or not cleavage reinitiation is predicted by the dynamic models.

Several factors that influence post-cleavage arrest predictions in dynamic models of the type employed in this study include (but are not limited to):
1. Dynamic initiation toughness of the vessel material,
2. Dynamic fracture toughness of the vessel material,
3. Pre- and post-cleavage ductile tearing (such as that observed in the HSST/PTSE-2 experiment),
4. Constitutive modeling and fracture parameters of the material (e.g., plasticity, strain-rate effects, etc.),
5. Geometric model of the crack (e.g., two-dimensional vs. three-dimensional representation of the propagating crack).

The differences in predictions of reinitiation of the arrested crack are predominantly controlled by the assumed toughness. This issue condenses to the relevance of the rate dependency shown in Fig. 9 to the realistic situations of interest.

Clarification of any one of the above issues represents a formidable research challenge, but the development of an effective model of the complete fracture event is dependent

upon substantial progress being made in several of these areas.

REFERENCES

1. R. D. Cheverton and D. G. Ball, Martin Marietta Energy Systems, Inc., Oak Ridge National Laboratory, "Probabilistic Fracture Mechanics Analysis of Potential Overcooling Sequences," pp. 263–306 in *Pressurized-Thermal-Shock Evaluation of the H. B. Robinson Nuclear Power Plant*, USNRC Report NUREG/CR-4183, Vol. 1 (ORNL/TM-9567/V1), September 1985.

2. R. D. Cheverton and D. G. Ball, Martin Marietta Energy Systems, Inc., Oak Ridge National Laboratory, *Pressurized-Thermal-Shock Evaluation of the Calvert Cliffs Unit 1 Nuclear Power Plant*, USNRC Report NUREG/CR-4022 (ORNL/TM-9408), September 1985.

3. R. D. Cheverton and D. G. Ball, Martin Marietta Energy Systems, Inc., Oak Ridge National Laboratory, *Preliminary Development of an Integrated Approach to the Evaluation of Pressurized-Thermal-Shock as Applied to the Oconee Unit 1 Nuclear Power Plant*, USNRC Report NUREG/CR-3770 (ORNL/TM-9176), May 1986.

4. *Code of Federal Regulations*, Title 10, Part 50, Section 50.61 and Appendix G.

5. U.S. Nuclear Regulatory Commission, Regulatory Guide 1.154, "Format and Content of Plant-Specific Pressurized Thermal Shock Safety Analysis Reports for Pressurized Water Reactors."

6. R. D. Cheverton and D. G. Ball, Martin Marietta Energy Systems, Inc., Oak Ridge National Laboratory, *OCA-P, A Deterministic and Probabilistic Fracture-Mechanics Code for Application to Pressure Vessels*, USNRC Report NUREG-3618 (ORNL-5991), May 1984.

7. R. H. Bryan et al., Martin Marietta Energy Systems, Inc., Oak Ridge Natl. Lab., *Pressurized-Thermal Shock Test of 6-in.-Thick Pressure Vessels. PTSE-2: Investigation of Low Tearing Resistance and Warm Prestressing*. USNRC Report NUREG/CR-4888 (ORNL-6377), 1987.

8. E. Smith and T. J. Griesbach, *Simulating the Effect of Pressure Plus Thermal Loadings on Crack Arrest during a Hypothetical Pressurized Thermal Shock Event*, PVP-Vol. 213/MPC-Vol. 32, pp. 41–46, Pressure Vessel Integrity, ASME, 1991.

9. D. J. Ayres et al., Combustion Engineering Inc., "Tests and Analyses of Crack Arrest in Reactor Vessel Materials," Final Report NP-5121M on EPRI Research Project 2180-3, April 1987.

10. *The American Society of Mechanical Engineers Boiler and Pressure Vessel Code*, Section XI, Rules for Inservice Inspection of Nuclear Power Plant Components, 1986.

11. D. J. Naus et al., Martin Marietta Energy Systems, Inc., Oak Ridge National Laboratory, *Crack-Arrest Behavior in SEN Wide Plates of Quenched and Tempered A533 Grade B Steel Tested Under Nonisothermal Conditions*, NUREG/CR-4930 (ORNL/TM-6388), August 1987.

12. C. W. Schwartz, Martin Marietta Energy Systems, Inc., Oak Ridge National Laboratory, *Crack Speed Relations Inferred from Large SEN Specimens of A533B Steel*, NUREG/CR- (ORNL/Sub/79-7778/9), to be published.

13. R. J. Fabi and D. J. Ayres, Combustion Engineering, Inc., "Calculating Dynamic Crack Arrest by Static Analogy," Final Report NP-6223 on EPRI Research Project 2455-14, March 1989.

14. K. J. Bathe, *ADINA – A Finite Element Program for Automated Dynamic Incremental Nonlinear Analysis*, Massachusetts Institute of Technology Report 82448-1 (1975, revised 1978).

15. B. R. Bass et al., "Applications of ADINA to Viscoplastic-Dynamic Fracture Mechanics Analysis," *Computers and Structures*, Vol. 32, No. 3/4, pp. 815-824, 1989.

16. J. Jung and M. F. Kanninen, "An Analysis of Dynamic Crack Propagation and Arrest in a Nuclear Pressure Vessel Under Thermal Shock Conditions," *Journal of Pressure Technology*, Vol. 105, pp. 111-116, May 1983.

17. M. F. Kanninen et al., "Preliminary Analysis of Japanese Wide-Plate Dynamic Crack Propagation-Arrest Experiments," subcontract report from Battelle-Columbus Laboratories to Oak Ridge National Laboratory, December 1983.

18. T. Kanazana, S. Machida, T. Teramoto and H. Yoshimura, "Study on Fast Fracture and Crack Arrest," *Experimental Mechanics*, Vol. 21, No. 2, pp. 78–88, February 1981.

19. B. R. Bass, C. E. Pugh, J. G. Merkle, D. J. Naus, and J. Keeney-Walker, "Fracture Analyses of Heavy-Section Steel Technology Wide-Plate Crack-Arrest Experiments," *Fracture Mechanics: Nineteenth Symposium, ASTM STP 969*, T. A. Cruse, Ed., American Society for Testing and Materials, Philadelphia, pp. 691–723, 1988.

20. D. J. Naus et al., Martin Marietta Energy Systems, Inc., Oak Ridge National Laboratory, "High-Temperature Crack-Arrest Behavior in 152-mm-Thick SEN Wide Plates of Quenched and Tempered A533 Grade B Class 1 Steel," U. S. Nuclear Regulatory Report NUREG/CR-5330 (ORNL/TM-11083), April 1989.

21. S. T. Rolfe and J. M. Barsom, *Fracture and Fatigue Control in Structures: Applications of Fracture Mechanics*, Prentice-Hall Inc., Englewood, N.J., 1977.

22. W. O. Shabbits, "Dynamic Fracture Toughness Properties of Heavy Section A533 Grade B Class 1 Steel Plate," Westinghouse R&D Center, WCAP-7623, HSST Technical Report No. 13, December 1970.

23. J. H. Giovanola and R. W. Klopp, SRI International, Menlo Park, Calif., "Viscoplastic Stress-Strain Characterization of A533B Class 1 Steel," USNRC Report NUREG/CR-5066 (ORNL/Sub/87-SA193/1), September 1989.

24. J. F. Kalthoff, "On the Measurement of Dynamic Fracture Toughness – A Review of Recent Work," *International Journal of Fracture*, Vol. 27, pp. 277298, 1985.

25. J. G. Merkle et al., "Fracture Mechanics Analysis and Investigations," Heavy-Section Steel Technology Program Quarterly Program Report July-September 1982, NUREG/CR-2751, Vol. 3, pp. 3–7, January 1983.

DISCLAIMER